# Supporting analysis for WCLL Test Blanket System safety

M. D'Onorio[(a)], D.N. Dongiovanni[(b)], I. Ricapito[(c)], J. Vallory[(c)], M.T. Porfiri[(b)], T. Pinna[(b)], G. Caruso[(a)]

a) Sapienza University of Rome, Dep. of Astronautical Electrical and Energy Engineering (DIAEE), C.so Vittorio Emanuele II 244, Rome, Italy
b) ENEA CR. Frascati, UTFUS-TECN, Via Enrico Fermi, 45, 00044 Frascati, Rome, Italy
c) Fusion for Energy, Carrer Josep Pla, 2, Torres Diagonal Litoral B3, 08019 Barcelona, Spain

## Abstract

The Water-Cooled Lithium Lead Breeding Blanket is one of the most promising concepts to be used as a key component in fusion power devices. It provides tritium breeding and nuclear power conversion and extraction. Before its integration in a DEMO plant, a testing phase is required to gain data on both thermal and neutronic performances. For this purpose, a Test Blanket System is currently under conceptual design and will be integrated into dedicated ITER equatorial ports. Early insight on the safety performance of the Test Blanket System remains an essential element for integrating into ITER, and accident analysis is one of its critical components. Preliminary safety studies have been performed in the framework of Safety And Environment (SAE) work package of the EUROfusion consortium program to support the design and the integration of the Water-Cooled Lithium Lead Test Blanket System into ITER. At the present conceptual design phase, these studies are tailored to give insight on the effects of some parameters, such as postulated initiating event timing, plasma termination system or valves intervention, and possible safety provision implementation. A MELCOR model of the Water-Cooled Lithium Lead Test Blanket System has been developed, and two accident scenarios have been studied: an ex-vessel LOCA inside the port cell and a loss of flow accident because of pump seizure. The impact of mentioned parameters on accident evolution and consequences is investigated in support of the safety logic definition.

Keywords: *Safety, ITER, WCLL, Test Blanket System, Test Blanket Module, MELCOR*

## 1. Introduction

One of the main engineering performance goals of the International Thermonuclear Experimental Reactor (ITER) is to test and validate design concepts of tritium breeding blankets relevant to a power producing reactor. The European Water Cooled Lithium Lead Test Blanket Module (WCLL TBM) is one of the blanket concepts to be tested in ITER as a possible candidate for a future application in the EU-DEMO reactor [1][2]. The WCLL TBM and related ancillary systems are currently undergoing a conceptual design phase managed by the Fusion for Energy (F4E) agency, which is responsible for the design, development, and integration of European TBM [3] [4]. Preliminary safety studies to support the design and the integration of the WCLL TBSs into ITER are performed in the framework of the Safety And Environment (SAE) work package of the EUROfusion consortium program [5]. In this conceptual design phase, preliminary safety scoping studies were tailored to gain insight into the impact and efficiency of specific safety logic design options and settings during the occurrence of reference accident scenarios.

Corresponding author:
matteo.donorio@uniroma1.it

Accident sequences to be investigated were identified on the basis of most representative accident initiators (Postulated Initiating Events (PIE)) as highlighted by a Failure Mode and Effect Analysis (FMEA) [6]. Among PIEs identified by FMEA, the initial efforts have been focused on ex-vessel events: an ex-vessel Loss Of Coolant Accident (LOCA) in the ITER port cell; and a Loss Of Flow Accident (LOFA).

The ex-vessel LOCA accident PIE is a double-ended guillotine break of the TBM inlet Water Coolant System (WCS) pipe during an ITER plasma burn phase, resulting in water loss into the port cell. Concerning the LOFA, the initiating event is a WCS pumps seizure.

Such events can evolve into in-vessel LOCA events if not appropriately managed. A few parameters may impact such accident evolution, such as time available for the intervention of Fast Termination Plasma System (FTPS) or isolation valve closure. Therefore, different values have been considered for such parameters to gain insight on the system response. Also, from an investment protection perspective, the grace time available in case of PIE occurrence in the proximity of the End of Plasma Pulse (EPP) has been studied to check the possibility of early handling such cases without the direct intervention of safety devices.

The methodology followed to study this accident sequence follows the one used for previous helium-cooled TBM concepts [7]: Helium Cooled Lithium Lead (HCLL) [8] and Helium Cooled Pebble Bed (HCPB) [9], for which safety studies have already been conducted [10].

The fusion version of the MELCOR code (ver. 1.8.6) [11][12] has been used to evaluate accident consequences for the selected scenario. MELCOR was chosen because of its capability of consistently simulating coolant thermal-hydraulic behavior and radionuclide and aerosol transport in reactor cooling systems during severe accident scenarios. MELCOR can also predict structural temperatures (e.g., First Wall (FW), blanket, divertor, and vacuum vessel) resulting from energy produced by radioactive decay heat and oxidation reactions to test if safety margins are respected during the accident sequences.

## 2. WCLL TBM and WCS reference design

ITER TBMs are made for testing the viability of tritium breeding technology necessary for future fusion power plant self-sufficiency in tritium fuel. Several TBM concepts are being developed for such purpose, including a breeding material (containing lithium isotopes) and a neutron multiplier material (e.g., Be, Pb) to favor tritium production through neutron capture reactions with lithium nuclei. A heat removal system is also associated with TBMs to keep the system within suitable operating conditions during plasma pulses.

The WCLL-TBM concept is characterized by the use of Reduced Activation Ferritic Martensitic (RAFM) steel EUROFER-97 as a structural material, the eutectic LiPb as tritium breeder and neutron multiplier, and water as coolant [13].

The TBM will be placed in a dedicated ITER equatorial port. The TBMs FW will act as a plasma-facing component, although it will be recessed of 120 mm compared to the ITER shield modules FW, to avoid major heat loads transients which are expected in ITER [14]. As shown in Figure 1, TBMs are inserted in pairs within a water-cooled stainless-steel frame acting as an interface with the VV/port structure and providing thermal isolation between the TBMs and the ITER shield blanket. This frame, together with two TBM-Sets, forms the so-called TBM Port Plug (PP).

In Figure 2, an overview of the main components of WCLL TBM is shown. The current conceptual design phase foresees a TBM box formed by a C-shaped first wall covering the upper, lower, and

Corresponding author:
matteo.donorio@uniroma1.it

frontal parts of the TBM. The two sides are closed by two non-cooled Side Caps (SC), while the rear part is closed by four steel plates delimiting manifolds for the distribution and collection of the water coolant inside the breeder blanket inside the first wall [15]. Vertical rectangular cross-section channels cool the TBM-box first wall. Vertical and horizontal non-cooled stiffening plates are provided to withstand the internal pressurization in case of an accident. The resulting stiffening grid divides the box interior into 16 separate channels called Breeder Units (BUs). Lithium-lead flows for allowing extraction of the tritium in the port cell area. In each cell, up to four radial-toroidal Double Wall Tubes (DWTs), with an internal diameter of 8 mm and a global thickness of 2.75 mm, are inserted and welded to a common backplate.

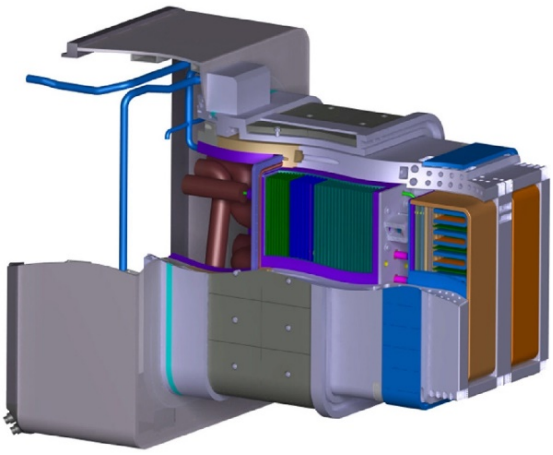

**Figure 1 - Global view of the two EU TBM sets and the port plug frame assembly [3]**

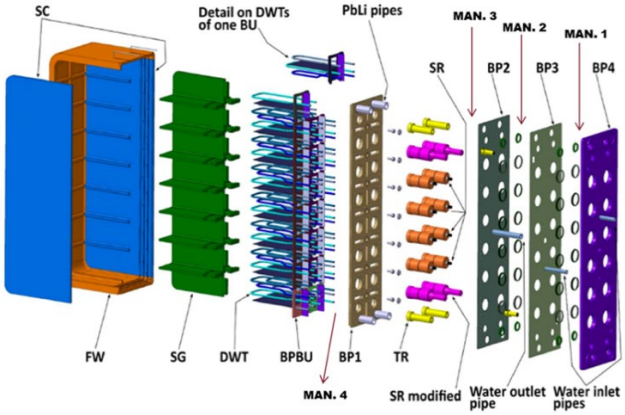


**Figure 2 - Exploded view of the WCLL TBM [13]**

A single water-cooling circuit cools down separately the FW and the Breeder Zone (BZ). The thermal power produced within the WCLL-TBM is removed through pressurized water circulating in cooling channels embedded in the FW facing the plasma and in the BZ DWT immersed in the liquid breeder. In nominal conditions, the circuit is operated at 15.5 MPa with inlet/outlet temperatures of 568.15/601.15 K and mass flow rates of ~1.79 kg/s in the FW and ~1.48 kg/s in the BZ [13].

The WCS loop is mainly installed in the Tokamak Water Cooling System (TWCS) area on building level four; the rest of the components, including the TBM, are placed in the port cell at building level one. The corresponding port cell Vertical Shaft (VS) hosts the pipelines connecting the two parts of the system [16]. The WCS conceptual design was developed following the analogy with the EU-DEMO WCLL Breeding Blanket (BB) Primary Heat Transfer System (PHTS). However, a single cooling circuit for both FW and BZ has been designed because of the reduced thermal power produced in the TBM box [17]. Its main functions are to transport thermal power from WCLL-TBM to the Component Cooling Water System (CCWS) heat sink and to provide a confinement barrier for water and radioactive products. The WCS consists of a primary loop feeding the TBM set and a secondary loop to avoid contaminated water entering the CCWS exceeding the allowable radioprotection limits for this system [18].

The WCS is mainly based on two separate heat exchangers: an economizer (HX-1) placed at the center of the loop and a heat exchanger between primary loop and secondary loop (HX-2). The WCS primary loop has an eight shape, with the TBM installed on the hot side and the pumping system located in the low temperature branch. Being the CCWS heat sink temperatures far lower than the TBM temperatures, an economizer has been installed in the WCS primary loop to avoid excessive temperature difference between the heat exchanger sides and then reducing the thermal stresses.

Corresponding author:
matteo.donorio@uniroma1.it

The source power of the WCLL TBM during the normal plasma pulse operation is 723 kW. The nuclear heating after the plasma shutdown has been scaled from decay heat data of the HCLL TBM [8] because of the unavailability of decay heat data for the WCLL concept.

## 3. Development of the TMB, WCS, and ITER environments MELCOR models

The equipment, components, and pipework constituting the WCLL TBM, related WCS, and coupled ITER systems outlined in the previous section have been mapped onto a MELCOR model using a suitably chosen set of Control Volumes (CV) connected by FLow paths (FL), Heat Structures (HS) conveying materials thermal properties and Control Functions (CF) to model system operating conditions and working logic.

The nodalization approach used to study this accident sequence follows the same methodology used for previous helium-cooled TBM concepts reported in [7]. The design intent of the MELCOR model of the WCLL TBM is to provide the necessary level of details whilst achieving a reasonable transient calculation time. For this purpose, the MELCOR model has been developed by maintaining all the geometrical data (hydraulic diameters, flow areas, lengths, elevations, material thickness, heat transfer surfaces) related to fluid flow paths and internal structures. The fluid and steel inventories are also strictly maintained. The volumes, flow areas, and channel lengths are based on measurements from the CAD model [15]. Water was chosen as a simulation working fluid. Given the MELCOR code limitation allowing for a single working fluid allowed in the same simulation, the Lithium-Lead flowing into the breeding zone has been simulated with equivalent heat structures.

A scheme of systems considered in MELCOR nodalisation is proposed in Figure 4. Given the purpose of exploring TBM thermal response to accidental transient loads, such a system model was developed in relatively greater detail with respect to other systems in scope, as described in the following.

An overview of the nodalisation of the WCLL-TBM is provided in Figure 3. Figure 3 (left) is a poloidal section view of the TBM nodalisation, showing breeding heat structure (BZ) and Stiffening Plates (SP) for each breeding unit level, but also FW, Side Walls (SW), and manifold models. Figure 3 (bottom right) is a toroidal section of a single breeding unit mainly focused on showing DWTs CVs and the thermal coupling between SC and breeding structures. To limit the size of the model, the two parallel columns of breeding units divided by the vertical stiffening grid (SG) in Figure 2, have been collapsed into a single column of BU modelling equivalent CVs, FLs and HSs such that at each elevation the power, coolant flow, heat transfer and inventory of both columns are suitably represented. In MELCOR, a slightly simplified model of the FW/SW coolant channels has been developed, neglecting the details of the true two-traverse FW/SW flow path geometry. This was due to the restriction that heat structures such as those representing the FW and SW, may contact only two hydraulic volumes (one on each of its two boundaries). Therefore, in the developed nodalisation, all FW channels are assumed to flow from the bottom to the top of the FW vertical structure. It is an approximation with respect to the real FW design in which channels are in counter-current one other two. The FW/SW squared channels are collapsed in three control volumes (CV603, CV604, CV605), as shown in Figure 3. FW/SW heat structures have been divided into two separated structures; conduction and thermal radiation heat transfer between the heat structures is modelled using MELCOR user-defined control functions ('FUN1'). The three water manifolds have been modelled with three equivalent CVs with associated flow paths and 4 rectangular HSs. Manifold containing LiPb is modelled with a single heat structure together with the breeding unit backplate and BP1 (Figure 2).

Groups of three or four DW channels connected in parallel into a single breeding unit are represented by single MECOR components. Following this approach, the BZ of the overall TBM box results

Corresponding author:
matteo.donorio@uniroma1.it

constituted by a stack of eight levels over posed one each other. The top and bottom of these volumes contain six DWTs; the central ones contain eight DWTs. The thermal-hydraulic modelling of DWTs consists of 24 CVs components, 3 for each BU, and 32 flow paths. They model the U-shape tube on the horizontal plane (radial – toroidal – radial). Each MELCOR modelled BU is bounded: laterally by the SCs, on the top/bottom by the horizontal stiffening plates. The presence of horizontal baffle plates has been neglected because LiPb is not treated as fluid; thus, its flow path inside BU cannot be modeled. The LiPb and SPs region modeling consists of 46 different heat structures that are thermally linked to the adjacent ones using FUN1s. The division in 2 radial LiPb HS layers is needed to obtain a temperature of LiPb behind the FW that is consistent with the value obtained from thermo-mechanical analyses. Since the breeder is not treated as fluid convective heat transfer coefficient was neglected, and only the conductive heat transmission was considered. This assumption is also justified by the low velocity of LiPb inside the BZ. By neglecting the convective heat transfer coefficient, the FW structure experience a higher temperature during the accident sequence, making the analysis conservative.

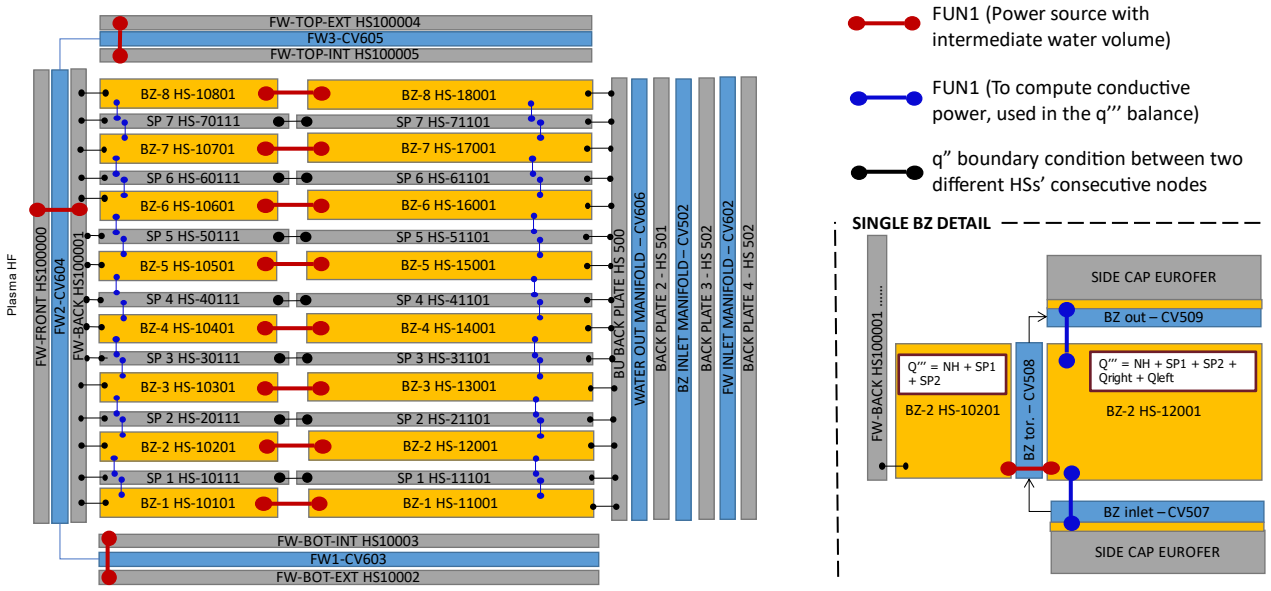


**Figure 3 - WCLL TBM control volumes and heat structure nodalisation**

Figure 4 shows a schematic representation of the WCS MELCOR nodalisation. The WCS pipeline routing and initial conditions for pressure, temperature, and power have been taken from the WCS reference design [19]. The MELCOR model of the WCS has been developed together with the RELAP5 mod3.3 [20] model described in [18]. A total number of 143 1-D CVs have been modeled to correctly simulate the WCS pipe volume and components maintaining all the elevations. WCS model includes pipe forests, delay tanks, vertical shafts, surge line, pressurizer, economizer, HX with secondary loop, CCWS, pump system, coolant purification system, and the electrical heater. Fluid flows between CVs have been modeled via associated flow paths. Loss coefficients were calculated and inserted in FL components to simulate the right pressure drops associated with valves, filters, tees, elbows, and abrupt area changes. The WCS pipe walls are modelled using cylindrical heat structures with the thermal properties of 316 stainless steel. A heat structure is assigned to each pipework CV node. As a conservative assumption, an adiabatic boundary condition is imposed on the outer side of each HS to neglect heat transfer with the environment.

The ITER port plug has been included in the model to account for the heat exchange by thermal radiation from TBM depending on relative mutual temperature differences. The TBM is in fact surrounded by the internal walls of the PP frame with an approximate gap between 7 mm and 9 mm.

Corresponding author:
matteo.donorio@uniroma1.it

The MELCOR PP model consists of 8 CVs, connecting FL, and 8 HSs modelling the stainless-steel frame structure. Radiative heat transfer between the PP and TBM and conduction between different PP frames, has been modelled using a series of FUN1 functions.

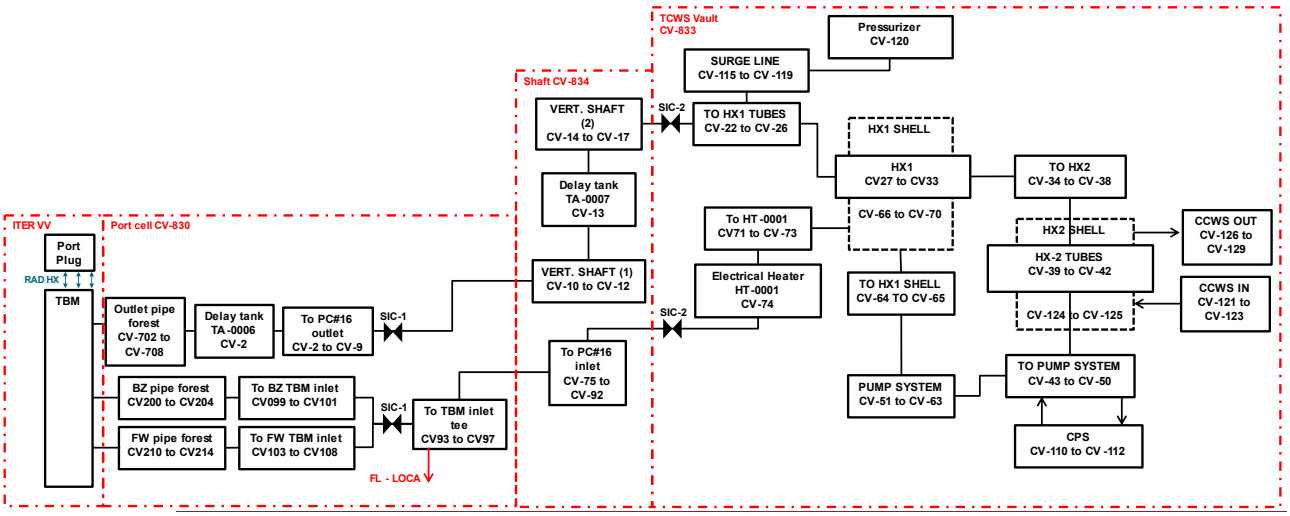


**Figure 4 – The MELCOR WCS model nodalisation scheme**

The relevant ITER environments have been modelled with MELCOR together with the Ventilation and Detritiation System (VDS) to assess fluid leakage and the transport of radionuclides within the Port Cell (PC), TCWS vault, gallery, and VS. All these volumes are nodalized with single CV components. The associated FLs are used to model ventilation flows, leakage flows and engineered pressure relief paths according to the ITER safety data list [21]. Heat structures simulating the tokamak building have also been modeled. Figure 5 shows a schematic representation of the ITER rooms and detritiation system MELCOR model.

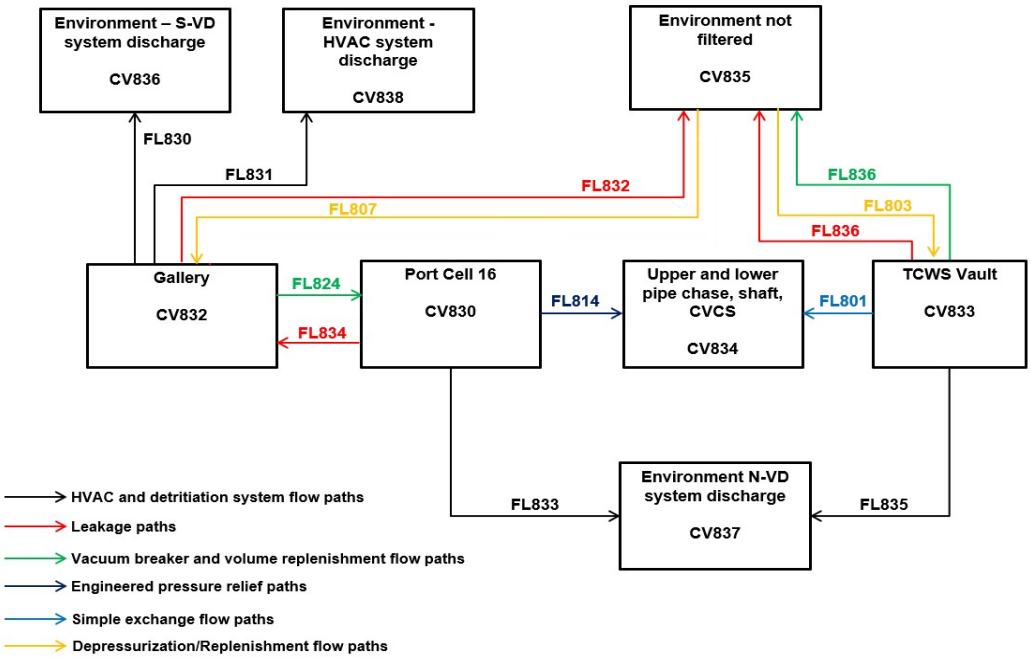


**Figure 5 – MELCOR nodalisation of the ITER rooms and detritiation system**

## 4. Accident selection and modelling

Concerning the ex-vessel loss of cooling accident, the postulated event is a double-ended guillotine break of the 3" TBM inlet WCS pipe during an ITER plasma burn phase resulting in loss of water

Corresponding author:
matteo.donorio@uniroma1.it

into the port cell. Break location has been set on the inlet line of WCS from TBM set, outside glove box, upstream the SIC-1 safety isolation valves (on the PC door side) to maximize water inventory potentially released in the port cell (Figure 4).

The initial part of the transient is a blowdown of the pressurized water circuit into the port cell due to the double-ended rupture of the TBM inlet WCS cold pipe, with consequential pressurization of the PC. The pressure relief device in the port cell opens towards the cooling system room through the service shaft. The tritiated water contained in the WCS enters the port cell and the cooling system room. The VDS connected to the port cell, TCWS vault, gallery, and cryostat space room are modelled to cover the pressure and leak conditions. The accident occurs during ITER's normal operating state when a pulsed plasma regime is foreseen. Plasma pulse pattern foresees the full plasma power to be reached within 60 s and, after 450 s of flat-top, the power is ramped down in 200 s. The dwell time between two consecutive plasma pulses is 1090 s.

Accident evolution after PIE occurrence and related consequences in terms of released inventories to containment strictly depend on the foreseen safety provisions and implemented logic. In fact, the amount of inventory released will depend on the isolation logic and settings defined for the SIC1 and SIC2 valves (Figure 4). Conversely, the possible evolution of ex-vessel LOCA into an in-vessel LOCA, resulting from TBM FW failure mainly depends on the time of shutdown of the plasma reaction. Plasma reaction termination can either occur by pulse sequence ending (200 s in normal operation) or forced by the activation of a SIC-2 class fast (order of 3 s) FTPS. The activation of the FTPS is assumed to produce a disruption with relatively higher (with respect to normal plasma pulse ending) thermal loads on plasma-facing components, hence possibly determining TBM FW failure. The intervention of FTPS and valves is triggered when the pressure in the pressurizer is 80% of the nominal pressure.

Concerning the LOFA, the initiating accident is a WCS pumps seizure. The WCS layout used for this analysis foresees one pump normally operating and a backup pump operating in parallel upon first pump failure. Therefore, in order to postulate the loss of flow accident due to pump seizure, either a common cause failure for both pumps is to be postulated or the main pump seizure shall be followed by a “fail to start” event for the backup pump. The PIE is assumed to occur at the beginning of the plasma pulse flat top.

As reported in Table 1, different case scenarios have been studied to study the relative impact of safety logic implementation for both LOCA and LOFA. A scoping analysis was performed for mentioned variables, resulting in different accident sub-scenarios. In particular, some cases have been investigated by varying the time of shutdown of the plasma reaction, the role of SIC safety isolation valves, the effects of plasma shutdown thermal loads, and the available grace time in case of FTPS activation. In such perspective, the time of PIE occurrence has also been varied considering different times during the plasma pulse: the beginning of plasma flat top (60 s); 50 s before the end of plasma flat top (460s); at the end of plasma flat top (510s). In the performed analyses, a simulation time of 0.0 s corresponds to the beginning of the plasma ramp-up phase. In Table 1, reporting the CASE matrix overview, the parameter “Time of PIE” is the time from the beginning of the plasma pulse. Since the figures showing the results focus on the transient pattern after PIE occurrence, where needed curves have been normalized to have PIE at time 0 s.

Corresponding author:
matteo.donorio@uniroma1.it

**Table 1 - Selected accident scenarios. (Pressure nominal (Pn))**

| PIE | CASE ID | Time of PIE | FTPS | SIC1 Valve closure | SIC2 Valve closure | Investigation GOAL |
|---|---|---|---|---|---|---|
| Ex-vessel LOCA | 1 | 460 s | -- | -- | EPP (710 s) | Insight on FW grace time |
| | 2 | 60 s | -- | -- | EPP (710 s) | |
| | 3 | | -- | 80% Pn | 80% Pn | |
| | 4 | 460 s | 80% Pn | -- | 80% Pn | Insight on FTPS impact. |
| LOFA | 1 | 60 s | -- | -- | -- | Insight on FW grace time |
| | 2 | 60 s | Y (5s) | -- | -- | Insight on FTPS impact. |
| | 3 | 510 s | -- | Spurious closure at 510 s | -- | Investigate the impact of not trigger FTPS during ramp-down. |

## 5. Analyses results

### 5.1 Loss of Coolant Accident Case 1

A short (2000 s) period has been modeled to establish the appropriate steady-state temperatures before the occurrence of PIEs. In Case 1 and Case 4, the LOCA scenario initiating event occurs 50 s before plasma flat top end (460 s), while in Case 2 and Case 3, the PIE occurs at the beginning of the flap-top phase. The LOCA results in a release of water in the port cell environment and subsequent pressurization. As shown in Figure 6, the pressure peak of 124 kPa is reached in the PC immediately after the LOCA. Thus, if any valve is closed during the plasma pulse, plasma power's effects on PC pressurization are negligible. As specified in Table 1, in Case 4 the FTPS is triggered when the pressure in the pressurizer is 80% of nominal pressure (around 5.2 s after the PIE). Moreover, it was assumed that the closure of SIC-2 valves occurs 3 s after FTPS. The closure of SIC-2 valves reduces the total inventory of water discharged in the PC, allowing for a faster depressurization of PC volume. In Case 1 and Case 2, pressure in the PC returns lower than that in gallery volume around 150 s after the PIE, when PC pressure is 99.9 kPa. However, in Case 4, despite SIC-2 valve closure, the depressurization process leading the PC to 99.9 kPa is slightly slower than Case 1 and Case 2 and occurs in around 190 s. This is due to the slightly smaller density of gas in PC, which reduces the leak rate toward penetration with PC, which is governed by volumetric flow rate assumed to be 20% of PC volume per day, for a differential pressure of 300 Pa. Concerning Case 3, the rapid closure of both SIC 1 and SIC 2 valves reduces the amounts of water discharged in PC and the sub-atmospheric pressure condition is restored around 25 s from the PIE. As shown in Figure 7, in all cases, pressure in the TCWS vault always remains below 110 kPa, and venting toward the external environment is never required.

Corresponding author:
matteo.donorio@uniroma1.it

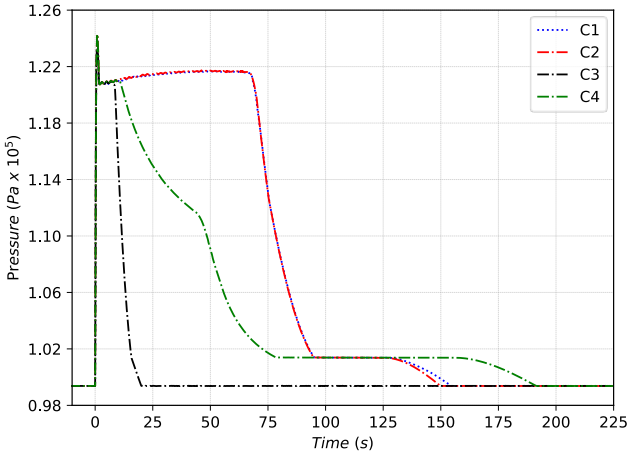


**Figure 6 - Pressure in Port Cell (PIE at 0 s)**

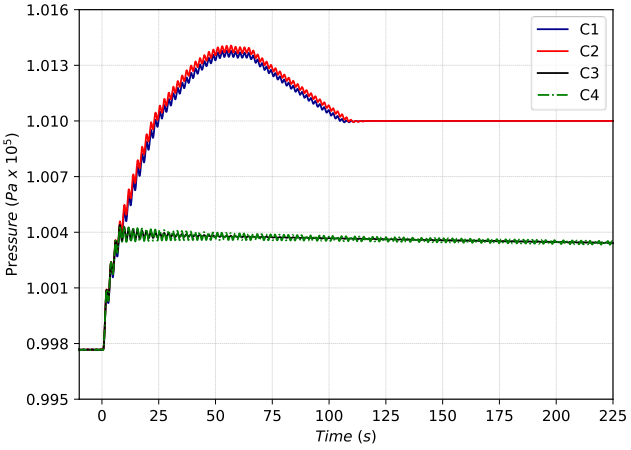


**Figure 7 – Pressure in TCWS Vault (PIE at 0 s)**

The total mass of steam and water discharged into the PC from the WCS is reported in Figure 8. In both Case 1 and Case 2, characterized by a late/non closure of SIC-2 valves, the total inventory of water released in the PC is around 2.4 tons. Among these, 98% is lost during the first 50 s of the accident sequence. In Case 3 the prompt closure of SIC valves reduces the total inventory discharged to PC to 460 kg, while in Case 4, around 1,022 kg are released. In all the simulations, the relief panel connecting the PC to vertical shafts volume (FL814) acts 0.4 s after the PIE, when the pressure in PC is 20 kPa higher than that in shafts. In Case 1 and Case 2, the relief panel remains open for about 67 s, while in both Case 3 and Case 4, after 8.0 s from the PIE, the relief panel is closed. As shown in Figure 9, in Case 1 and Case 2, around 356 kg of steam from the PC penetrates the gallery volume (CV832) toward FL820, which opens if the pressure difference between the PC and the gallery is higher than 1.5 kPa. Instead, in Case 3 and Case 4, only 55 kg of steam are moved toward the gallery volume.

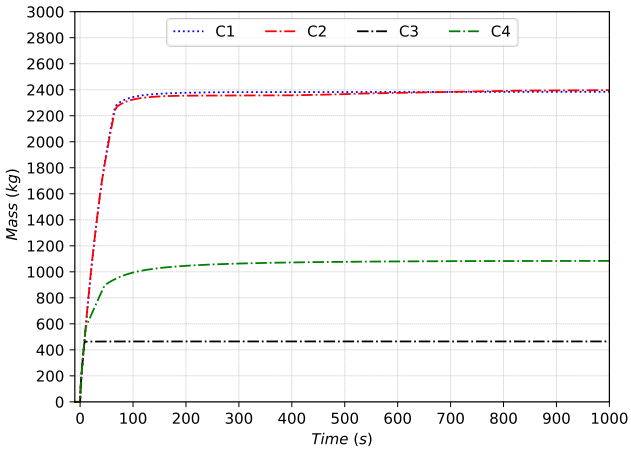


**Figure 8 – Inventory discharged from guillotine break to Port Cell (PIE at 0 s)**

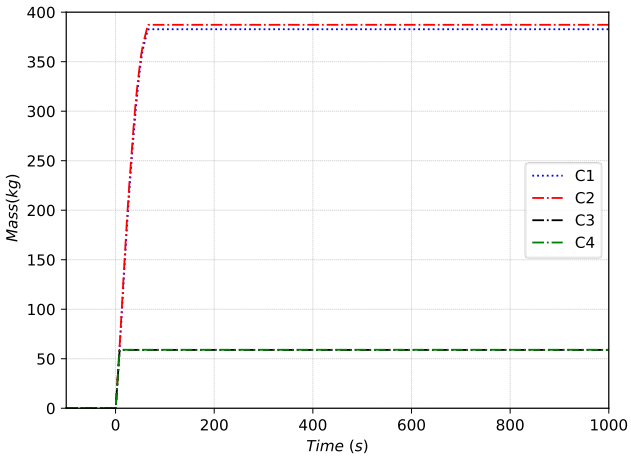


**Figure 9 - Mass from PC to Vertical Shafts (PIE at 0 s)**

The occurrence time of the LOCA PIE event with respect to the plasma pulse phase has also been varied to investigate the possible role of reverse water flow from the pressurizer and steam generator in cooling down the TBM after the PIE. The water reverse flow toward FW channels is shown in Figure 10. Suddenly, after the LOCA, a reverse water mass flow rate up to 6 kg/s is reached in all cases. This allows the cooling of TBM vertical FW in the early stages after the LOCA. In Case 3, in

Corresponding author:
matteo.donorio@uniroma1.it

which the SIC-1 valve close, the MFR instantaneously goes to 0.0, while in the other, it slowly decreases to zero.

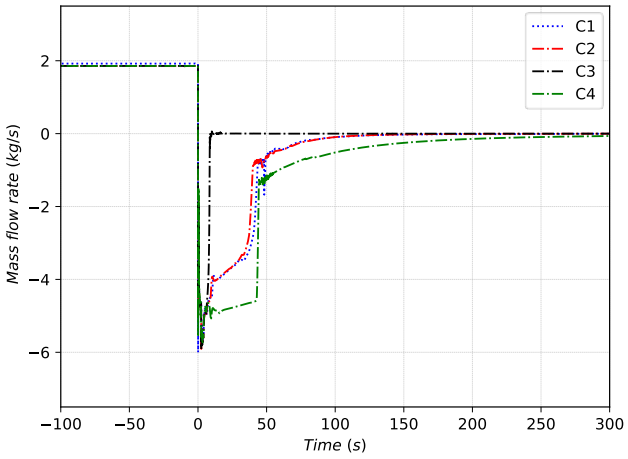


**Figure 10 – Water Mass Flow Rate entering FW volume (CV604, PIE at 0 s)**

As the blowdown continues, the circuit's heat removal capability is degraded, and the TBM undergoes a temperature excursion. The long-term transient of the FW and BZ is depicted in Figure 11 for Case 1 and 4, and in Figure 12 for Case 2 and Case 3. In Case 1, the FW temperature rises from 657 K at 460 s (PIE) to reach a peak of 1028 K at 625 s during the rump-down phase of the plasma pulse. A similar temperature trend is achieved in the BZ with a maximum temperature of 964 K.

Case 4 is characterized by the intervention of the FTPS, which causes a temperature spike of FW temperature up to 850 K. In Case 2 and Case 3, the temperature excursion of FW and BZ structures is higher compared with those of others the other two cases. This is mainly because of the strongly conservative assumptions made to give insight on FW structure behaviors during the transient. The PIE is supposed to occur at the beginning of the plasma flat-top phase (60 s), and the plasma continues to burn until the EPP. The maximum temperature reached by the FW in Case 2 is 1677 K at 517 s from the PIE; the BZ temperature (behind the FW structure) follows the same trend with a maximum temperature of 1545 K.

In Case 3, the intervention of SIC valves causes a higher temperature peak in the FW and BZ structures, with a maximum value of 1766 K and 1635 K, respectively.

In all the simulations, after the temperature peak, both FW and BZ temperatures start to fall. In Case 1, this temperature drop is aided by a thermal radiation heat loss rate of around 6.0 kW at 710.0 s (EPP) from the TBM FW to the ITER machine. While in Case 2 and Case 3, the radiative power peak toward ITER internals could reach 70 kW. The radiative heat transfer between TBM FW and ITER internal components is assumed as well as the heat loss by thermal radiation from the TBM side caps to the PP. The average rate of heat loss by thermal radiation to the Port Plug is ~2.3 kW, evaluated over the entire simulation period.

Corresponding author:
matteo.donorio@uniroma1.it

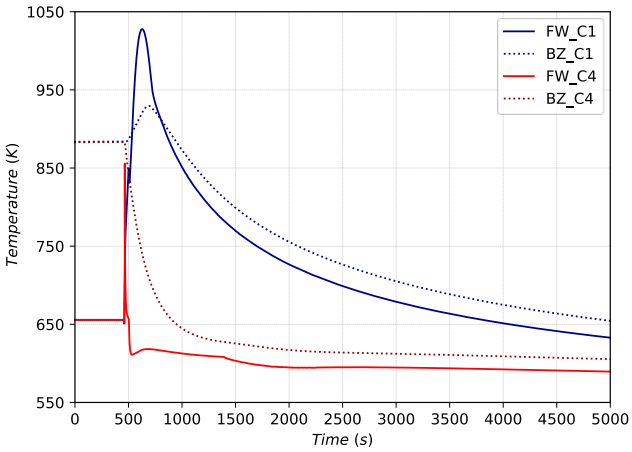


**Figure 11 – FW and BZ temperature transient in CASE 1 and CASE 4**

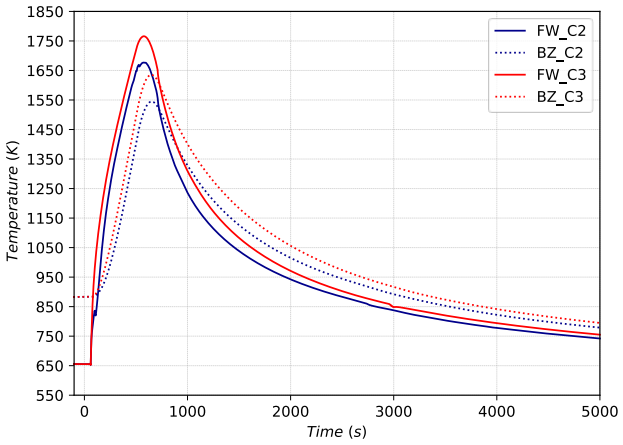


**Figure 12 – FW and BZ temperature transient in CASE 2 and CASE 3**

## 5.2 Loss of Flow Accident

In LOFA Case 1 and Case 2, the PIE occurs at t=60 s, at the beginning of plasma pulse flat-top. The loss of coolant flow causes a rapid reduction in the rate of heat removal from the TBM, leading to temperature excursion of the TBM FW and pressurization of the WCS and TBM coolant. In Case 3, the PIE has been supposed to occur at t = 510 s, at the end of plasma pulse flat-top, together with a spurious closure of SIC-1 valves. Note that while pump failure events are commonly falling into an incident frequency category (f > ~$10^{-2}$/year), this last case would move the accident frequency to significantly lower values since considering an additional (1.E-10/yea).

The pressurization trends for WCS pressurizer and FW volume are shown in Figure 13 and Figure 14, respectively. In Case 1, WCS and TBM systems pressure increases to 17.7 MPa (setpoint for PORVs opening) in around 60 s. Steam is discharged from the pressurizer into a small suppression relief tank through the PORVs and, in case of PORVs failure, through the Safety Relief Valves (SRVs) triggered at a higher pressure setpoint. The total amount of steam discharged from the pressurizer into the relief tank is around 90.0 kg. In Case 2 and Case 3, the maximum pressure inside the TBM is around 165 bar, and the intervention of PORVs is never required.

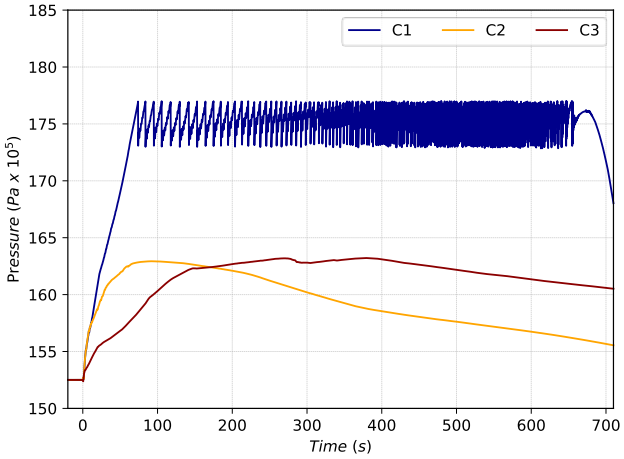


**Figure 13 – Pressure transient in WCS pressurizer (PIE at 0 s)**

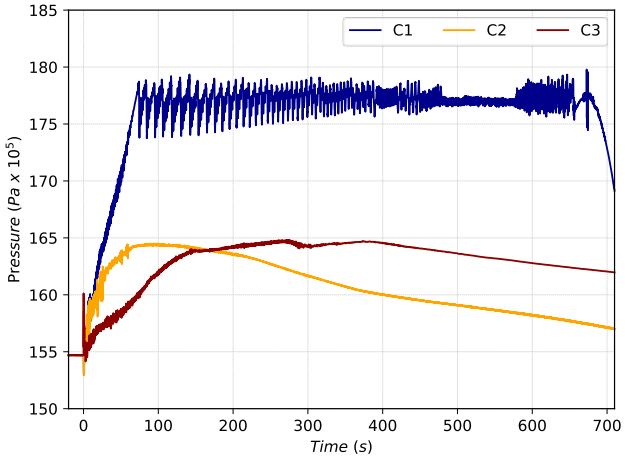


**Figure 14 - Pressure transient in TMB FW volume(CV604, PIE at 0 s)**

The temperature transient of the FW structure for Case 1 is shown in Figure 15. The FW temperature rises from 657 K at 60.0 s to reach the maximum temperature of 1175 K at t=540 s, 480 s after the

Corresponding author:
matteo.donorio@uniroma1.it

PIE. After that, the FW temperature starts to fall, reaching 630 K at the EPP. A similar temperature trend is achieved in the BZ with a maximum temperature of 1185 K (Figure 16).
Temperature transient for the FW for Case 2 and Case 3 is shown in Figure 17 and Figure 18, respectively. In Case 2, the FTS is activated 5 s after the PIE (conservatively taking into account the time to detect the drop in current absorption by WCS Pump < 70% nominal and actuation), and the occurrence of a plasma disruption on the TBM FW is simulated. A peak temperature of around 850 K on the first layer of the HS. In Case 3, because of further reduced cooling capacity deriving from the spurious closure of the SIC-1, the FW structure experienced a maximum temperature of around 1000 K.
Note that the poloidal temperature profile of the FW has not been evaluated, being the FW plasma-facing structure simulated with a single vertical HS component.

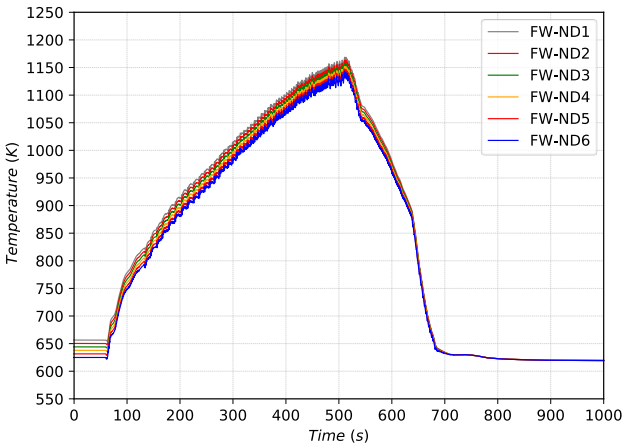


**Figure 15 – FW temperature transient in all HS nodes for LOFA CASE 1**

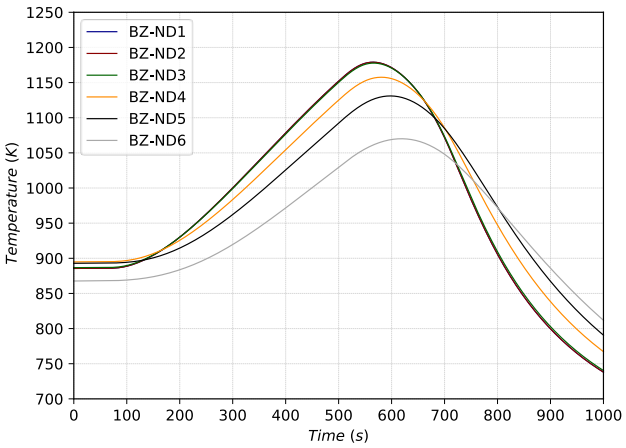


**Figure 16 - BZ temperature transient in all HS10401 nodes for LOFA CASE 1**

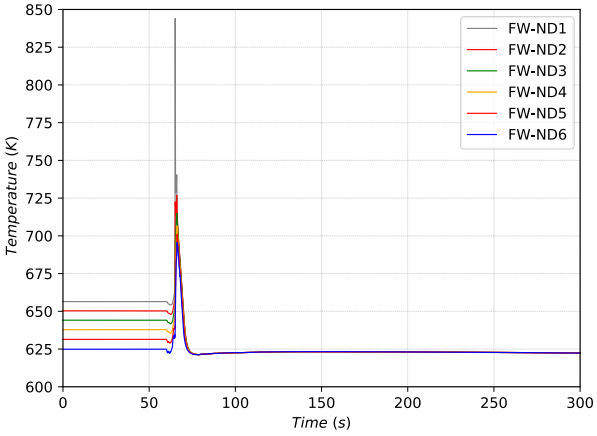


**Figure 17 – FW temperature transient in all HS nodes for LOFA CASE 2**

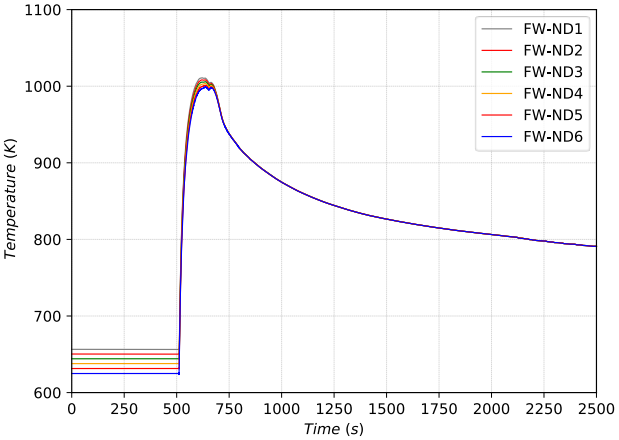


**Figure 18 – FW temperature transient in all HS nodes for LOFA CASE 3**

## 6. Summary and conclusions

A preliminary MELCOR model has been developed to perform safety studies on ITER WCLL TMB. The model includes a detailed representation of the TBM box, WCS, Tokamak Building, and Port Plug frame. The breeder material within the TBM has been simulated with equivalent heat structures. The MELCOR input deck has been developed following a modular scheme to facilitate future model enhancement. Parametric studies on the time of occurrence of the initiating events and activation of

Corresponding author:
matteo.donorio@uniroma1.it

safety provisions has been performed on two PIEs (ex-vessel LOCA event, LOFA event) regardless of the impact on resulting accident category classification.

Preliminary results of LOCA analyses highlight that the TBM-FW can reach temperatures up to around 1700 K for PIE occurring at the beginning of the flat-top phase. Note that it is still to be assessed which combined load conditions (structure temperature point combined with the related pressure load) would result in EUROFER structural loss of integrity. In fact, depending on such design value, the considered accidents could potentially evolve either into an in-box LOCA or in-vessel LOCA event.

Since most of the inventory is released within the first 50 s, the bounding effects of SIC-1 valves closure during the LOCA transient are limited. Since a large part of the inventory is released few seconds after the LOCA, a delayed intervention of SIC-2 valves does not ensure a reduction of releases. The occurrence time of the LOCA PIE event with respect to the plasma pulse phase has been varied to investigate the possible role of reverse water flow from the pressurizer and steam generator in cooling down the TBM after the PIE. Aside from defense in depth considerations that ultimately manage the consequences of studied accidents, these outcomes open the possibility of adopting design solutions providing initial management of such events (or small leak events) with machine protection class provisions. Such provision could prevent TBM re-pressurization, eventually resulting in in-Vessel/in-box LOCA events.

The impact of fast termination plasma system has also been preliminarily investigated by modelling the effects of a plasma disruption on the TBM FW. The disruption causes an increase of around 200 K on the FW surface, comparable to the effect of around 100 s of full-power plasma.

Parameters' variation effect of LOFA transient on FW temperature appears less significant than the LOCA ones; however, PORVs and SRVs opening setpoint should be accurately chosen to reduce the mechanical stress on structures.

Note that FTPS system is an active safety system SIC-2 class. Its failure is more likely than for SIC-1 passive systems (e.g., fail close isolation valves), so such parametric analyses also help gain insight into accident consequences in such a failure case. Besides that, the effectiveness/opportunity of its automated intervention during plasma phase end could be evaluated based not only on system parameters response but also on its possible impact on triggering in-vessel events. Aside from a consequence-bounding safety perspective that still holds in a safety demonstration assessment, in a machine protection perspective feedback to designers, the presented outcomes are meant to investigate the possibility of managing the accident through soft plasma ending strategies. While not substituting safety provision, such initial managing machine protection provisions could prove effective in specific conditions near plasma pulse end and scaling on the severity of actual initiating event possibly resulting in temporary limited loss of flows.

## 7. Acknowledgments

This work has been carried out within the framework of the EUROfusion Consortium and has received funding from the Euratom research and training programme 2014-2018 and 2019-2020 under grant agreement No 633053. The views and opinions expressed herein do not necessarily reflect those of the European Commission.

Corresponding author:
matteo.donorio@uniroma1.it

## 8. List of Abbreviations

| | |
|---|---|
| BB | Breeding Blanket |
| BU | Breeder Units |
| BZ | Breeder Zone |
| CCWS | Component Cooling Water System |
| CF | Control Functions |
| CV | Control Volumes |
| DWTs | Double Wall Tubes () |
| EPP | End of Plasma Pulse |
| F4E | Fusion for Energy |
| FL | FLow paths |
| FMEA | Failure Mode and Effect Analysis |
| FTPS | Fast Termination Plasma System |
| FW | First Wall |
| HCLL | Helium Cooled Lithium Lead |
| HCPB | Helium Cooled Pebble Bed |
| HS | Heat Structures |
| ITER | International Thermonuclear Experimental Reactor |
| LOCA | Loss Of Coolant Accident |
| LOFA | Loss Of Flow Accident |
| PC | Port Cell |
| PHTS | Primary Heat Transfer System |
| PIE | Postulated Initiating Events |
| PP | Port Plug |
| RAFM | Reduced Activation Ferritic Martensitic |
| SAE | Safety And Environment |
| SC | Side Caps |
| SG | Stiffening Grid |
| SP | Stiffening Plates |
| SW | Side Walls |
| TBM | Test BlanketModule |
| TWCS | Tokamak Water Cooling System |
| VDS | Ventilation and Detritiation System |
| VS | Vertical Shaft |
| WCLL | Water Cooled Lithium Lead |
| WCS | Water Coolant System |

## 9. Reference


[1] L.M. Giancarli, "Overview of recent ITER TBM Program activities", *Fusion Engineering and Design*, **158** (2020), 111674, https://doi.org/10.1016/j.fusengdes.2020.111674

[2] G. Federici, et al., "An overview of the EU breeding blanket design strategy as an integral part of the DEMO design effort", *Fusion Engineering and Design*, **141** (2019), https://doi.org/10.1016/j.fusengdes.2019.01.141

[3] J. Vallory, et al., "Design activities toward the achievement of the conceptual phase of the EU-TBM sets", *Fusion Engineering and Design*, **109-111** (2016), pp. 1053-1057, https://doi.org/10.1016/j.fusengdes.2016.01.026

[4] I. Ricapito, et al., "Current design of the European TBM systems and implications on DEMO breeding blanket", *Fusion Engineering and Design*, **109-111** (2016), pp. 1326-1330, https://doi.org/10.1016/j.fusengdes.2015.12.034

[5] F. Romanelli, "Fusion Electricity – a roadmap to the realization of fusion energy", EFDA (2012), pp. 20-28, ISBN 978-3-00-0407



Corresponding author:
matteo.donorio@uniroma1.it

[6] T. Pinna, et. al., "Failure mode and effect analysis for the European test blanket modules", *Fusion Engineering and Design*, **83** (2008), pp. 1733-1737, https://doi.org/10.1016/j.fusengdes.2008.06.041
[7] D. Panayotov, et al., "Methodology for Accident Analyses of Fusion Breeder Blankets", *Fusion Engineering and Design*, **109-111** (2016), pp. 1574-1580, https://doi.org/10.1016/j.fusengdes.2015.11.019
[8] A. Grief, et al., "Qualification of MELCOR and RELAP5 models for EU HCLL TBS accident analyses", *Fusion Engineering and Design*, **124** (2017), pp. 1165-1170, https://doi.org/10.1016/j.fusengdes.2017.03.048
[9] X. Jin, et al., "Deterministic safety analysis of the reference accidental sequence for the European HCPB TBM system", *Fusion Engineering and Design*, **83** (2008), pp. 1759-1763, https://doi.org/10.1016/j.fusengdes.2008.06.018
[10] D. Panayotov, et al., "Status of the EU test blanket systems safety studies", *Fusion Engineering and Design*, **98-99** (2015), pp. 2201-2205, https://doi.org/10.1016/j.fusengdes.2014.12.016
[11] J. Merrill, et.al, "A recent version of MELCOR for fusion safety applications", *Fusion Engineering and Design*, **85** (2010), pp. 1479-1483
[12] R. O. Gauntt, et al., "MELCOR Computer Code Manuals vol. 1: Primer and Users" Guide Version 1.8.6, NUREG/CR-6119, vol. 1, Rev. 3, Sandia National Laboratory, (2005).
[13] J. Aubert, et al., "Design and preliminary analyses of the new Water Cooled Lithium Lead TBM for ITER", Fusion Engineering and Design, 160 (2020), 111921, https://doi.org/10.1016/j.fusengdes.2020.111921
[14] L.M. Giancarli, et al., "Overview of the ITER TBM Program", *Fusion Engineering and Design*, **87** (2012), https://doi.org/10.1016/j.fusengdes.2011.11.005
[15] R. Boullon, J. Aubert, "Definition of A WCLL Reference TBM Set design based on the WCLL BB Design – First CAD Model and Scoping Calculations", IDM Ref. EFDA_D_2N7CDT_v1.2 (2019)
[16] A. Aiello, et al. "Updated design and integration of the ancillary circuits for the European Test Blanket Systems", *Fusion Engineering and Design*, **146** (2019), pp. 27-30, https://doi.org/10.1016/j.fusengdes.2018.11.015
[17] C. Ciurluini, et al., "Thermal-hydraulic modeling and analysis of the Water Cooling System for the ITER Test Blanket Module", *Fusion Engineering and Design*, **158** (2020), 111709, https://doi.org/10.1016/j.fusengdes.2020.111709
[18] F. Giannetti, "Thermohydraulic analyses of WCS, CPS, Pb-Li loop, TRS: Methodology and Results", IDM ref. EFDA_D_2P99TK v1.0 (2020)
[19] A. Tincani, et al., "WCLL-TBS System Design Description Document - part on the four main Ancillary Systems", EUROfusion internal deliverable EFDA_D_2NTPVX v1.1 (2019)
[20] F. Giannetti, T. D'Alessandro, C. Ciurluini, Development of a RELAP5 mod3.3 version for FUSION applications. DIAEE Sapienza Technical Report D1902_ENBR_T01 Rev. 01.
[21] L. Topilski et al. Safety Analysis Data List (SADL), Version 2.0, ITER IDM number ITER_D_3ETKYX v. 2.0, 2011.
[22] D. Dongiovanni, "Accident Analysis Specifications for ITER WCLL TBM", IDM EFDA_D_2NA6ZP v1.1 - T001-D002 (2020)

Corresponding author:
matteo.donorio@uniroma1.it